The Plant Journal (2015) 82, 903–914

A two-component enzyme complex is required for dolichol biosynthesis in tomato1

Megan I. Brasher[a], Liliana Surmacz[b], Bryan Leong[c], Jocelyn Pitcher[a], Ewa Swiezewska[b], Eran Pichersky[c] and Tariq A. Akhtar[a],[1]

[a]*Department of Molecular and Cellular Biology, University of Guelph, Guelph, Ontario, N1G2W1;*
[b]*Institute of Biochemistry and Biophysics, Polish Academy of Sciences, 5A Pawinskiego Street, 02-106 Warsaw, Poland;*
[c]*Department of Molecular and Cellular and Developmental Biology, University of Michigan, Ann Arbor, Michigan 48109, USA*

[1]For Correspondence: Tariq A. Akhtar Telephone: (519) 824 4120 ext. 54794
Fax: 519-837-1802 E-mail: takhtar@uoguelph.ca

Running Title : Dolichol biosynthesis in tomato

Key words: *cis*-prenyltransferase, Nogo-B receptor, polyisoprenoid, polyprenol, endoplasmic reticulum, *Solanum lycopersicum*

SUMMARY

Dolichol plays an indispensable role in the N-glycosylation of eukaryotic proteins. As proteins enter the secretory pathway they are decorated by a ‘glycan’, which is preassembled onto a membrane-anchored dolichol molecule embedded within the endoplasmic reticulum (ER). Genetic and biochemical evidence in yeast and animals indicate that a *cis*-prenyltransferase (CPT) is required for dolichol synthesis, but also point to other factor(s) that could be involved. In this study, RNAi-mediated suppression of one member of the tomato CPT family (SlCPT3) resulted in a ~60% decrease in dolichol content. We further show that the involvement of SlCPT3 in dolichol biosynthesis requires the participation of a distantly related partner protein, designated as CPT binding protein (SlCPTBP), which is a close homolog of the human Nogo-B receptor. Yeast two-hybrid and co-immunoprecipitation assays demonstrate that SlCPT3 and its partner protein interact, *in vivo*, and that both SlCPT3

and SlCPTBP are required to complement the growth defects and dolichol deficiency of the yeast dolichol mutant, *rer2Δ*. Co-expression of SlCPT3 and SlCPTBP in yeast and in *E. coli* confirmed that dolichol synthase activity strictly requires both proteins. Finally, organelle isolation and *in vivo* localization of fluorescent protein fusions showed that both SlCPT3 and SlCPTBP localize to the endoplasmic reticulum, the site of dolichol accumulation and synthesis in eukaryotes.

INTRODUCTION

It is estimated that approximately 50% of the eukaryotic proteome undergoes posttranslational modification (Apweiler *et al.,* 1999). One of the most prominent of these modifications is N-glycosylation, which critically affects protein folding, subcellular localization and activity. As proteins are translocated across the endoplasmic reticulum (ER) membrane and enter the secretory pathway, a 14-sugar glycan is transferred to specific asparagine residues on the nascent polypetide within the ER lumen (Schenk *et al.,* 2001; Ruiz-May *et al.,* 2012). The glycan is assembled onto a membrane-anchored, long-chain unsaturated lipid, known as dolichol (Chojnacki and Dallner, 1988; Hemming 1992). Although the enzymes involved in glycan assembly are well characterized, the biosynthesis of dolichol remains poorly understood.

Dolichol belongs to a larger class of compounds known as polyisoprenoids (Swiezewska and Danikiewicz 2005). These hydrophobic polymers originate from the universal five-carbon (C5) isoprene building blocks, isopentenyl diphosphate (IPP) and its isomer dimethylallyl diphosphate (DMAPP). In plants, two distinct pathways provide these two polyisoprenoid precursors: The mevalonate (MVA) pathway produces IPP in the cytosol while the methylerythritol phosphate (MEP) pathway produces IPP and DMAPP in the plastid (Lange et al., 2000; Bick and Lange 2003; Kirby and Keasling 2009). Plant polyisoprenoids broadly fall into one of two classes, the dolichols and polyprenols (Fig. 1). Polyprenols typically range in size from C25-C65, while dolichols are longer (C70-C95) and are fully saturated at the terminal α-isoprene unit (Surmacz and Swiezewska 2011). While dolichol is present in nearly all plant tissues, the short (C25-C40) and medium chain (C40-C65) polyprenols are primarily associated with roots and leaves, respectively (Kurisaki *et al.,* 1997; Skorupinska-Tudek *et al.,* 2008; Bajda *et al.,* 2009). Surprisingly, very little is known about plant polyprenol synthesis and physiological function.

Polyisoprenoid synthesis can be viewed as a two-step process. First, the condensation of up to three IPP units with DMAPP generates a *trans*-prenyl diphosphate precursor. This

intermediate acts as a scaffold onto which a *cis*-linked chain of IPP units is then attached. The class of enzymes known as *cis*-prenyltransferases (CPTs) elongate the *trans*-prenyl diphosphate intermediate with a *cis*-linked linear polymer of IPP units (Liang *et al.*, 2002; Kharel and Koyoma 2003). Bacterial, yeast and mammalian CPTs are well established. In bacteria, CPTs synthesize medium-chain polyisoprenoid diphosphates ('undecaprenol', C50-C55), which serve as lipid carriers in cell wall peptidoglycan biosynthesis (Bugg and Brandish 1994). In animals and yeast CPTs produce dolichol, which, as described above, plays an indispensable role in the post-translational modification of proteins (Sato *et al.*, 1999; Shridas *et al.*, 2003). By contrast, comparatively little is known about plant CPTs, although clear genomic evidence exists for multi-gene CPT families throughout the plant kingdom (Akhtar *et al.*, 2013).

Defects in dolichol biosynthesis lead to a range of congenital disorders in animals that are typically characterized by aberrant protein glycosylation. The involvement of a specific CPT in dolichol biosynthesis was first identified in yeast via the *rer2Δ* mutant strain, which is defective in ER protein sorting. The orthologous human CPT was subsequently identified by sequence similarity and shown to compliment the *rer2Δ* mutant (Shridas *et al.*, 2003; Endo *et al.*, 2003). However, *in vitro* evidence for dolichol synthesis in animals, yeast and plants has only been demonstrated with crude microsomal preparations (Sakaihara *et al.*, 2000; Rush *et al.*, 2010; Harrison *et al.*, 2011), spurring speculation that other factors present on the ER membrane may contribute toward its synthesis. The first evidence that dolichol synthesis may involve an additional protein factor resulted from a genetic screen for leaf wilting phenotypes in *Arabidopsis* (Zhang *et al.*, 2008). In this ethyl methanesulfonate-mutagenized population the causal gene was identified as LEW1 (*leaf-wilting1*) and shown to encode a distantly related CPT-like protein. Strikingly, the LEW1 mutant exhibited a ~85% reduction in leaf dolichols. Subsequent studies in animals showed that the knockdown of the orthologous protein, known as the Nogo-B receptor (NgBR), also results in a dolichol deficiency, as well as a robust decrease in CPT activity and a broad reduction in protein N-glycosylation (Harrison *et al.*, 2011). However, neither LEW1 nor NgBR were able to compliment the yeast dolichol *rer2Δ* mutant on their own.

In this study we further examined the relationship between the plant CPTs implicated in dolichol biosynthesis and the enigmatic role of LEW1/NgBR in this process. Using tomato as our model, we show that a member of the CPT gene family, SlCPT3, interacts with the tomato LEW1 ortholog. Both of these proteins were required to fully compliment the yeast *rer2Δ* mutant, restore microsomal CPT activity, and dolichol synthesis. Finally, expression of

the two proteins in *E. coli* demonstrated that they form a two-component enzyme complex that synthesizes dolichol, *in vitro*.

RESULTS

The evolution of CPT and CPT-related proteins

An earlier analysis of the tomato CPT gene family revealed that plants contain multiple CPTs, unlike the majority of other eukaryotes and prokaryotes (Akhtar *et al.,* 2013). An expanded search for CPT-like proteins was performed in order to examine the evolutionary relationships between LEW1 and NgBR with predicted CPTs. Sequences (Figure S2) were retrieved from GenBank and the Joint Genome Institute Genome Portal (Phytozome) and phylogenetic analysis was performed using MEGA5 (Tamura *et al.,* 2011). This search identified a gene from tomato on chromosome 6 (not linked to any other tomato CPT gene) that encodes a protein with 47% identity to LEW1 and 21% identity to NgBR, and which we designated as CPT-Binding Protein (SlCPTBP) for reasons described below. Our phylogenetic analysis demonstrated that CPTs fall into four distinct groups: Groups 1 and 2 are comprised of dicot and monocot-specific CPTs. Group 3 contains the CPTs of prokaryote origin and group 4 contains the animal and yeast CPTs that are implicated in dolichol biosynthesis and at least one member from every plant that was surveyed. The LEW1, NgBR, ScNus1p (from *Saccharomyces cerevisiae*), SlCPTBP and orthologous proteins from other plant species form a fifth, distinct group (Fig. 2A), indicating that this branch of the family diverged from *bona fide* CPTs prior to the split of the plant and animal lineages.

Analysis of the domain architecture of representative CPTs and related proteins from all five groups revealed four characteristic features. First, the plant CPTs in groups 1 and 2 contain N-terminal extensions that are predicted to encode organellar targeting sequences. Second, the five conserved regions including the dimer interface and the six amino acid residues that are implicated in substrate binding and/or catalysis are present in all CPTs from groups 1, 2 and 3 (Kharel and Koyama 2003). Third, the CPTs in group 4, which are believed to participate in dolichol synthesis, lack N-terminal extensions and the conserved E213 residue (numbering based on the *E. coli* enzyme). Lastly, the CPT-related proteins in group 5 contain a truncated CPT domain, lack many of the conserved residues found in CPTs, have predicted N-terminal signal peptides and encode proteins with two predicted transmembrane domains (Fig. 2B).

RNAi-mediated knockdown of SlCPT3

To explore the involvement of SlCPT3 in tomato dolichol synthesis, we performed RNAi-mediated knockdown and measured SlCPT3 expression and total polyisoprenoid contents in the transgenic plants. In three independent RNAi lines, SlCPT3 gene expression was reduced by approximately 60% (Fig. 3A). Although transgenic plantlets were recovered that exhibited a higher degree of SlCPT3 knockdown, they did not survive to maturity. The polyisorenoid content of the RNAi lines that could be propagated were analyzed by HPLC, and in these lines, dolichol (15-17 isoprene units long) levels were reduced on average by 60% (Fig. 3B). The medium chain polyprenols (~9 isoprene units; C55) in these plants, which constitute a major portion of the total polyisoprenoid content in plant leaves, was unaffected. Among RNAi lines that did not exhibit a significant degree of SlCPT3 mRNA knockdown, dolichol levels were unchanged relative to wild type plants (Supplemental Figure S1). Compared to wild type tomato plants, RNAi lines with reduced SlCPT3 gene expression exhibited a pleiotropic phenotype, which included mottled, wilted leaves and stunted growth, which is consistent with the indispensable role that dolichol serves (Fig. 3C).

Functional complementation of the yeast *rer2Δ* dolichol mutant

The yeast *rer2Δ* mutant is deficient in dolichol synthesis and exhibits slowed growth at elevated temperatures. Survival of the yeast mutant is ensured by a second CPT gene that is cryptically expressed only during stress and stationary phase growth, therefore providing a unique platform to test for dolichol synthase activity of heterologously expressed proteins. Accordingly, we introduced SlCPT3 as well as SlCPTBP into the *rer2Δ* mutant, alone or together (using the native RER2 promoter for both), and assessed growth at the non-permissive temperature. The native RER2 gene, used as a positive control, was able to restore the growth of *rer2Δ* at 37°C. Neither SlCPT3, SlCPTBP, nor the expression vector alone completely rescued the growth defect of *rer2Δ*. However, when SlCPT3 and SlCPTBP were co-expressed growth was restored to equivalent levels as the control (Fig. 4A).

To confirm that the restoration of growth in the *rer2Δ* mutant by the co-expression of SlCPT3 and SlCPTBP was due to dolichol synthesis, we first isolated microsomal membranes from the various *rer2Δ* mutant strains and assayed for CPT activity. Microsomal membranes were incubated with FPP and 14C-IPP and the reaction products were resolved by reverse-phase TLC in order visualize polyprenoids of various sizes. In strains expressing the native RER2 gene, long chain polyisoprenoids (C75-90) which are the typical size of dolichols, were detected (Fig. 4B). Strikingly, the same enzymatic products were detected in assays with microsomes from the *rer2Δ* strain expressing both SlCPT3 and SlCPTBP, yet not with strains

expressing either protein alone or the expression vector. Next, we analyzed the polyisoprenoid content of the various *rer2Δ* strains by HPLC. Yeast cells expressing SlCPT3, SlCPTBP, or the vector alone accumulated similar amounts of short and medium chain (< 60 carbons in length) polyisoprenoids, whereas *rer2Δ* strains cells expressing the native RER2 or both SlCPT3 and SlCPTBP together accumulated identical long chain (75-85 carbons in length) polyisoprenoids that were identified as dolichols, based on comparison to authentic standards (Fig. 4C).

The SlCPT3 and SlCPTBP proteins interact to form a functional dolichol synthase

One possible explanation for the production of dolichols in *rer2Δ* strains expressing both SlCPT3 and SlCPTBP is that they associate together in an enzyme complex. We therefore tested for *in vivo* interactions between the two proteins using two independent approaches. First, yeast two-hybrid assays were performed by co-expressing SlCPT3 and SlCPTBP as GAL4-activating domain (AD) and GAL4-DNA binding domain (BD) fusion proteins in the yeast PJ69-4A strain, respectively. In this system, protein-protein interactions drive the GAL4-responsive expression of the auxotrophic markers, His and Ade (Fig.5A). Cells containing both SlCPT3 and SlCPTBP fusion proteins were able to rescue the *His*/*Ade* auxotrophy of the PJ69-4A yeast strain, indicating that they interact *in vivo*. On the other hand, cells expressing the 'empty' AD or BD in place of either fusion protein were unable to grow. We next examined this interaction *in planta* by introducing SlCPT3-Myc and SlCPTBP-FLAG tagged versions of the proteins into tobacco leaves and then performed co-immunoprecipitation assays. The SlCPT3-Myc protein was detected in SlCPTBP-FLAG immunoprecipitates, indicating that indeed these two proteins interact in a plant system (Fig. 5B). The interaction was specific, as SlCPT3-Myc was not detected in the absence of SlCPTBP-FLAG from tobacco leaf protein extracts.

An alternative explanation as to why both proteins are required to synthesize dolichol in the yeast *rer2Δ* strain is that SlCPT3 converts an intermediate compound that is produced by SlCPTBP into dolichol, or vice versa. This possibility was tested by performing a dialysis experiment in which desalted *E. coli* extracts expressing SlCPT3 and/or SlCPTBP were incubated with FPP and 14C-IPP in dialysis chambers that were separated by a 5 kDa molecular weight cutoff membrane that allows the passive diffusion of polyisoprenoid substrates, intermediates and products, but not proteins. Enzymatic products were extracted and separated by radio-TLC to assess their relative size (Fig. 5C). The TLC plate was then divided into zones according to the retardation (*Rf*) value and radioactivity in each zone was

quantified by scintillation counting. When SlCPT3 and SlCPTBP were incubated in separate chambers with all the necessary substrates to synthesize dolichol, long chain polyisoprenoids (C75-C90) were not detected. However, in chambers containing extracts that were co-expressing both proteins dolichols were formed, which freely diffused to neighbouring chambers that were incubated without any protein. Interestingly, when extracts expressing each protein individually were mixed and assayed for CPT activity, dolichol formation was not detected.

Subcellular localization of SlCPT3 and SlCPTBP

In eukaryotes, the synthesis and accumulation of dolichol is known to occur on the ER membrane. We therefore tested if both SlCPT3 and SlCPTBP localize to the ER, *in planta*, by transiently expressing C-terminal mCherry fusions of both proteins in *Arabidopsis* protoplasts that express an ER-GFP marker (Nelson *et al.,* 2007). Both SlCPT3-mCherry and SlCPTBPmCherry fluorescence was observed in these protoplasts and it largely co-localized with the fluorescence associated with the ER-GFP marker (Fig. 6A-F). Curiously, the mCherry fluorescence associated with SlCPTBP exhibited an additional punctate pattern that did not colocalize with the ER marker. When SlCPT3-GFP and SlCPTBP-mCherry fusion proteins were co-expressed in wild type *Arabidopsis* protoplasts, the two patterns of fluorescence completely overlapped (Fig. 6G-I).

To address the subcellular localization of both proteins more precisely, C-terminally tagged SlCPT3-Myc and SlCPTBP-FLAG were introduced into tobacco leaves and organellar membranes were separated by sucrose density gradient centrifugation and subjected to immunoblot analysis using antibodies against known organellar markers. A 25% to 55% linear sucrose gradient was utilized to separate membrane fractions that correspond to ER, Golgi, and plasma membranes and it was found that both SlCPT3-Myc and SlCPTBP-FLAG co-fractioned with the ER luminal marker, BiP (Fig. 6J). Interestingly, the SlCPTBP-FLAG protein also was detected in fractions associated with the Golgi marker, Arf1, suggesting that this protein may not be exclusively localized to the ER, as has been previously reported for the orthologous protein in animals (Harrison *et al.,* 2009). Taken together, SlCPT3 and SlCPTBP appear to co-localize to the site of dolichol biosynthesis on the ER membrane.

DISCUSSION

SlCPT3 and SlCPTBP form a 'dolichol synthase'

We provide evidence that SlCPT3 and SlCPTBP interact to form a two-component enzyme complex that synthesizes dolichol, *in vitro* and *in vivo*. The inability of SlCPT3 or SlCPTBP to synthesize dolichol or fully compliment the yeast *rer2Δ* mutant on their own implies that these proteins do not function as single enzyme subunits, but rather strictly require one another for activity. Dialysis experiments in which each protein was provided all of the necessary substrates for dolichol synthesis and then separated from its partner also rule out the possibility that SlCPT3 functions as an enzyme that acts on an intermediate produced by SlCPTBP, or vice versa. Although we cannot rule out the possibility of substrate channeling between the subunits, we instead propose that SlCPT3, and by extension all of the related CPTs in group 4 (Fig. 2A), participate in intersubunit allostery with the CPTBPs. These interactions likely alter the conformation and stability of each partner and are therefore necessary for forming the active enzyme. Although crystal structures for plant CPTs or CPTBPs are currently not available, three-dimensional homology models using the *E. coli* enzyme as a template can readily be constructed for all of the tomato CPTs except for SlCPT3 (Kang *et al.*, 2014), suggesting that the SlCPTBP is required for correcting folding and stability of the dolichol synthase. In support of this view, NgBR also appears to stabilize the mammalian CPT involved in dolichol synthesis, hCIT, since loss of NgBR leads to a marked reduction in hCIT protein levels and hCIT-mediated CPT activity (Harrison *et al.*, 2011). It is unlikely that a third protein factor is involved in the enzyme complex given that we were able to recapitulate dolichol synthesis enzyme activity in *E. coli* (Fig. 5C). Further support for a common function for NgBR and SlCPTPB (and AtLEW1) comes from the observation that these three proteins are more similar to each other than they are to any plant CPT protein (Fig. 2), indicating that the ancestral gene that gave rise to the genes encoding them diverged from the CPT family before the split between the animal and plant lineages. Bacterial genomes, on the other hand, do not encode any CPTBP orthologs and their CPTs function as autonomous homodimers without the requirement for accessory subunits (Liang *et al.*, 2002).

Several important questions still remain regarding the plant dolichol synthase enzyme complex itself, however. For instance, the details of the enzyme subunit stoichiometry, active site orientation, and kinetic parameters are still unknown. The origin and nature of the true initiator substrate for plant dolichol synthesis have also not been unambiguously determined. It has long been inferred from biochemical and structural studies that dolichol synthesis occurs with *trans*-FPP being extended with several units of IPP that are derived exclusively from the MVA pathway in the cytosol. However, stable isotope-assisted *in vivo* labeling studies with hairy root cultures of *Coluria geoides*, suggest otherwise (Skorupinska-Tudek *et*

al., 2008). In a series of elegant experiments it was demonstrated that polyprenols originating from the plastidlocalized MEP pathway provide the first ~12 isoprene units of dolichol; the polyprenol is then extended in the cytosol with the addition of IPP units that are derived entirely from the MVA pathway. Such a scenario would necessitate a continuous exchange of intermediates between the MVA and MEP pathways, for which there is precedent in plants (Bick and Lange, 2003; Dudareva *et al.*, 2005; Phillips *et al.*, 2008).

ER-targeting and orientation of dolichol synthase

One of the characteristic features of the CPT proteins that are implicated in dolichol biosynthesis (Group 4, Figure 2a) is that they lack typical organellar targeting sequences (Akhtar et al., 2013). This raises the question of how these CPTs localize to the ER membrane and participate in dolichol synthesis. Primary sequence analysis of the plant CPTBPs, on the other hand, predicts the presence of canonical N-terminal signal peptides. Therefore, we propose a model in which the CPTs are recruited to the ER through their interaction with CPTBPs and together form an enzyme complex that synthesizes dolichol on the ER membrane.

The orientation and topology of this two-component enzyme complex is still unclear, however. In animals, the orthologous CPTBP (NgBR) exists in at least two distinct conformations with the major portion of the protein orientated either towards the ER lumen or to the cytosol (Miao et al., 2006; Harrison et al., 2009, 2011). Whether the CPT accompanies its CPTBP partner to both sides of the ER membrane is not known. According to the current model, dolichol synthesis is initiated on the cytoplasmic leaflet of the ER and then transverses to the lumen during the completion of glycan assembly (Schenk et al., 2001). It is thought that a unique ‘flippase’ is involved in this transbilayer movement of dolichol (Sanyal et al., 2008; Sanyal and Menon, 2010), however no such enzyme has been identified in plants or animals. Therefore, it remains plausible that the dolichol synthase complex itself, or one of the two components, participates in the re-positioning of dolichol from the cytosolic to luminal leaflets of the ER during the glycan assembly process.

Results from our subcellular localization studies of SlCPTBP revealed that a minor portion of the protein appears localized outside of the ER. A punctate pattern of mCherry fluorescence was observed in Arabidopsis protoplasts that did not coincide with the ER–GFP marker and immunoblot analysis of subcellular fractions indicate that SlCPTBP partly localizes to the Golgi system. This observation is in agreement with studies in animals which have demonstrated that the orthologous CPTBP (NgBR) resides in both compartments

(Harrison et al., 2009). This raises the intriguing possibility that plant CPTBPs serve a secondary function, perhaps in cholesterol trafficking and homeostasis, as has been suggested in animal systems (Harrison et al., 2009).

Future implications

CPTs from all kingdoms of life have long been thought to function autonomously as homodimeric enzymes (Kharel and Koyama 2003). Our results challenge this view and suggest that all of the CPTs in the group 4 clade (Fig. 2A), which include at least one member from every eukaryote, strictly require an accessory protein subunit for activity. The homology-based association of the CPTs in group 4, however, does not necessarily ensure their involvement in dolichol synthesis, as these proteins could participate in the production of other long chain polyisoprenoids of biological importance. For instance, the CPTs that are implicated in the synthesis of *cis*-1,4-polyisoprene (natural rubber) also reside in this clade (Asawatreratanakul *et al.*, 2003; Schmidt *et al.*, 2010; Post *et al.*, 2012). Natural rubber (NR) is a high molecular weight (2 x 103 – 1 x 104 Da) polyisoprenoid that is derived from the polymerization of IPP units with an all *trans*-isoprene primer on the surface of 'rubber particles'. Although the precise mechanism for NR synthesis has not yet been elucidated, CPTBP orthologs have been identified in several rubber-producing plant species (Wahler *et al.*, 2012; Dai *et al.*, 2013; Qu *et al.*, 2015), which implies that a two-component enzyme complex may also be required for the synthesis of the world's most economically important polyisoprenoid.

EXPERIMENTAL PROCEDURES

Plant material and growth conditions

Wild type and transgenic *Arabidopsis thaliana* (Col-0), *Nicotiana benthamiana*, and tomato (MP-1) plants were grown in potting soil supplemented with Osmocote (Scotts) and maintained in growth chambers under a 16h photoperiod (150umol m−2s−1; mixed cool white and incandescent bulbs). Temperature was maintained at 23/18°C (day/night) and the relative humidity was 60%.

Chemical and reagents

Authentic polyprenol standards were obtained from Indofine chemical company (heptaprenol C35), Avanti Polar Lipids (polyprenol mixture C65-C105), and Cedarlane Labs (GPP, FPP, GGPP). Standards of dolichols were from the Collection of Polyprenols, Institute of Biochemistry and Biophysics Polish Academy of Sciences, Warsaw, Poland. Radiolabeled

14CIPP, 40-60 mCi (1.48-2.22 GBq mmol-1; 0.02 mCi ml-1) was obtained from PerkinElmer. TLC plates (RP18, Silica gel 200 micron, 20 cm x 20 cm) were obtained from Analtech. Antibodies for co-immunoprecipitation were Monoclonal ANTI-FLAG M2, clone M2 (Sigma-Aldrich), anti-*myc* (Life Technologies) and the secondary antibody was goat anti-mouse IgG**(**H+L)-HRP Conjugate (Bio-rad). For detection of organelle markers, anti-H+ATPase (plasma membrane H+ATPase), anti-BiP (lumenal-binding protein), anti-Arf1 (ADP-ribosylation factor 1), and goat anti-rabbit IgG (H&L), HRP conjugated secondary antibodies were obtained from Agrisera. Synthetic drop-out media lacking amino acids for yeast cultures were obtained from US Biological. All other chemicals were obtained from Sigma, BioBasic, or Fisher Scientific. All primers were synthesized by Integrated DNA Technologies and are listed in Supplemental Table S1.

Gene, cDNA isolation and phylogenetic analysis CPT sequences

The yeast RER2 gene was obtained by PCR using genomic DNA as a template prepared using the QIAamp DNA mini kit (Qiagen), according the manufacturer's instructions. The fulllength SlCPT3 and SlCPTBP cDNAs were isolated by RT-PCR. RNA was prepared from tomato leaf tissue with the EZNA plant RNA mini kit with on-column DNase digestion (Omega Biotek), reverse transcribed using Superscript II reverse transcriptase (Invitrogen) and used directly for PCR amplification with KOD hot start DNA polymerase (Novagen). PCR products were transferred to pGEM-T-Easy (Promega) and sequence-verified. CPT and CPT-related sequences were retrieved from GenBank and the Joint Genome Institute Genome Portal (Phytozome). The phylogenetic and molecular evolutionary analysis were conducted using MEGA version 5 (Tamura *et al.*,, 2011) and the tree was constructed using the neighbor joining method with bootstrap values from 1000 replicates.

RNAi mediated knockdown of SlCPT3 and quantitative RT-PCR

A 508 bp fragment of SlCPT3 (corresponding to base pairs 25-752) was ligated in a sense/antisense orientation into pRNA69 (Foster *et al.*, 2002) between the *XhoI*/*EcoRI* and *BamHI*/*XbaI* restriction sites, respectively. The hairpin cassette was transferred to the pZP212 binary vector and introduced into tomato by the University of Nebraska Plant Transformation Facility (http://biotech.unl.edu/plant-transformation) using agrobacterium-mediated transformation protocols. Gene expression was quantified using an Applied Biosystems 7300 Real-time PCR system (ABI) to detect SlCPT3 abundance and normalized to those for the tomato elongation factor 1α (EF1A). Total RNA extracted as described above and reverse transcribed to cDNA using the High Capacity cDNA Reverse Transcriptase Kit (ABI) with random hexamers. The PCR employed ABI universal cycling conditions using SYBR

GREEN PCR Master Mix (ABI) in a 25 μL reaction containing diluted (1:20) cDNA and 300 nM concentration of each primer. Expression values were calculated according to the 2-ΔCT method (Livak and Schmittgen 2001).

Extraction of polyisoprenoids from plants and yeast

Dolichols were extracted from yeast cells as described earlier (Surmacz et. al, 2014). After supplementation with an internal dolichol standard, yeast pellets were incubated in 10 ml of a hydrolytic solution (25 g KOH, 35 ml of water, brought to 100 ml with 99.8% ethanol) for 1h at 95 °C. Subsequently, lipids were extracted three times with hexane and pooled extracts were purified on silica gel 60 column using isocratic elution with 10% diethyl ether in hexane. Fractions containing polyisoprenoids were pooled, evaporated, dissolved in 2-propanol and analyzed by HPLC. For plant polyisoprenol extraction, leaf tissue was homogenized using Ultra-Turrax T25 (IKA Labortechnik) and lipids were extracted four times with chloroform:methanol:water (1:1:0.3) and incubated for 48 h at room temperature. The extracts were pooled and evaporated under nitrogen. Residual lipids were dissolved in 5 ml of a mixture containing toluene/7.5% KOH/95% ethanol (20:17:3 by vol.) and hydrolyzed for 1 h at 95 °C (Stone et al, 1967), than extracted with hexane, purified and analyzed as above.

Analysis of polyisoprenoids

Polyisoprenoids analysis was performed as described earlier (Skorupinska-Tudek *et al.,*, 2003). Extracted lipids were separated by HPLC (Waters) using a ZORBAX XDB-C18 (4.6 × 75 mm, 3.5 μm) reversed-phase column (Agilent, USA) eluted with a linear gradient from 0% to 100% methanol:isopropanol:hexane (2:1:1) in water:methanol (1:9) at a flow rate of 1.5 mL/min. Polyisoprenoids were detected by absorption at 210nm and quantified relative to authentic standards.

Functional Complementation

Yeast strain YG932 (*rer2Δ* mutant) (MATα rer2Δ::kanMX4 ade2-101 ura3-52 his3-200 lys2-801) was routinely cultured in yeast peptone dextrose media (YPD) at 23°C. The SlCPT3 gene was transferred to pYEP352, as described by Akhtar *et al.,* (2013). The native RER2 gene from yeast was ligated between the *Sma*I/*Hind*III sites of pYEP352 and the SlCPTBP open reading frame was transferred to the pRS423 vector between the *SmaI*/*BamHI* restriction sites. Yeast transformation was performed according to the method of Gietz and Schiestl (2007) and transformants were selected on 0.67% yeast nitrogen base without amino acids, 2% glucose and all necessary auxotrophic requirements, except uracil and/or histidine.

Yeast two-hybrid and co-immunoprecipitation assays

Yeast two-hybrid assays were performed using the Clonetech Matchmaker® GAL4 Two-Hybrid System 3 (Clontech). The open reading frames of SlCPT3 and SlCPTBP were ligated between the *Eco*RI/*Bam*HI sites of pGADT7 and the *Eco*RI/*Xho*I sites of pGBKT7 to create GAL4 activation- and DNA-binding domain fusions, respectively. Each construct was introduced into the yeast strain PJ69-4A (MATa trp1-901 leu2-3, 112 ura3-52 his3-200 gal4Δ gal80Δ LYS2::GAL1-HIS3 GAL2-ADE2 met2::GAL7-lacZ) and transformants were selected on synthetic drop out media lacking leucine and tryptophan, containing 0.67% yeast nitrogen base. Two-hybrid interactions were tested on the above media lacking histidine and adenine. For coimmunoprecipitation, C-terminally tagged CPT3-*myc* and CPTBP-FLAG fusion protein sequences were generated by PCR and ligated between the *Xho*I/*Eco*RI sites of pSAT4A. The expression cassette was then transferred between the unique *Sce*I site in the pZP-RCS2 binary vector. Leaves of four-week old *Nicotiana benthamiana* (tobacco) plants were infiltrated with cultures of *Agrobacterium tumefaciens* (LBA4404) carrying the above binary vectors. Protein extracts were prepared from ~1g of infiltrated tobacco leaf tissue in 2 ml of extraction buffer (50 mM Tris, pH 7.6; 150 mM NaCl; 1 mM EDTA; 1% Triton X-100; and 1x protease inhibitor cocktail (Sigma). Extracts were cleared of excess debris using a low spin at 5000 RPM for 10 minutes. Extracts were then further centrifuged at 12,000 x *g* for 10 minutes at 4°C. The supernatant was incubated at 4°C for 2 hours with Anti-Flag M2 Affinity Gel with gentle rocking and immunoprecipiated proteins were eluted according to the manufacturer's protocol. Samples were analyzed by SDS-PAGE and immunoblotting.

Subcellular Fractionation

Agrobacterium tumefaciens (LBA4404) expressing SlCPT3-Myc and SlCPTBP-FLAG were infiltrated into four-week old tobacco leaves and harvested 3 days after. Approximately 7 g of infiltrated tobacco leaf tissue was homogenized using a polytron in 25 ml of 50 mM Tris-HCl, pH 7.6, 10% glycerol, 5 mM EDTA, and 0.5 x protease inhibitor cocktail (Sigma). The homogenate was filtered through miracloth and the flow through was centrifuged for 10 minutes at 8,000 x *g* to remove excess debris. The microsomal fractions were prepared by centrifuging the supernatant at 120,000 x *g* for 1 hour using a SW Ti32 rotor (Beckman). The pellets were resuspended in 700 ul of 10 mM Tris-HCl, pH 7.6, 10% glycerol, 5 mM EDTA, and 1 x protease inhibitor cocktail (Sigma). The re-suspended pellets were loaded directly on top of a 12 mL, 25% to 55% [w/v] linear sucrose density gradient prepared in 10 mM Tris-HCl, pH 7.6, 5 mM MgCl2, 1 mM DTT, and 0.5 x protease inhibitor cocktail (Sigma). Centrifugation was performed using a SW28.1 rotor (Beckman) at 24,000 RPM for 16 hours. 500 ul fractions were subjected to immunoblot analysis.

Subcellular localization

The open reading frame of SlCPT3 and SlCPTBP were PCR-amplified and ligated between the *Sac*I/*Bam*HI sites of pSAT4A-mCherry-N1, creating an in-frame C-terminal fusion protein with mCherry. The constructs were mobilized into Arabidopsis protoplasts expressing an ER-localized GFP marker (Nelson *et al.,* 2007), according to the 'tape sandwich' method (Wu *et al.,*, 2009), and fluorescence was visualized 16 hours following transfection with a Leica SP5 laser scanning confocal microscope as previously described (Akhtar *et al.,* 2013). Spectral detection of mCherry and GFP fluorescence was captured between 465 nm and 495nm with the aid of a double dichroic 458/514 beam splitter.

Expression of recombinant SlCPT3 and SlCPTBP in *E. coli*

The open reading frames of SlCPT3 and SlCPTBP were amplified by PCR, A-tailed and then transferred into pEXP-5-CT/TOPO which permits recombinant protein expression from the T7 promoter. For co-expression of both proteins, a bicistronic message containing SlCPT3 and SlCPTBP separated by a ribosome binding site was created as follows: The SlCPT3 coding sequence was PCR amplified with C-terminal *Bam*HI/*Eco*RI sites and transferred to pEXP-5- CT/TOPO to create pCPT3CoEX. Similarly, the sequence for SlCPTBP was amplified with an N-terminal extension containing a ribosome binding site and then ligated between the *Bam*HI/*Eco*RI sites of pCPT3CoEX. Sequence-verified constructs were mobilized into BL21- CodonPlus (DE3)-RIPL *E. coli* cells, which were grown at 37°C in Luria-Bertani medium containing the appropriate antibiotics. When A600 reached 0.6, IPTG was added to a final concentration of 1 mM and incubation continued for 16 hours at 15°C.

Protein extraction and CPT enzyme assays

E. coli cells were disrupted by sonication in 50 mM HEPES, pH 8.0, 100 mM KCl, 7.5 mM MgCl2, 5 mM DTT, 5% glycerol [v/v], and 0.1% Triton-X-100 [v/v]. Soluble crude extracts were clarified with a 7500 g centrifugation for 10 minutes at 4°C and then desalted on PD-10 columns (GE Healthcare) equilibrated with 25 mM Tris-HCl at pH 8, 5mM MgCl2 and 5 mM DTT. Yeast cells were suspended in 50 mM Tris-HCl at pH 7.4, 0.25 M Sucrose, 5 mM EDTA, and 5 mM β-mercaptoethanol and then ruptured with glass beads. Cell lysates were centrifuged at 5000 g for 10 minutes at 4°C to remove unbroken cells and then further centrifuged at 100,000 g for 1 hour at 4°C to obtain crude microsomes. The post-100,000 g pellets were re-suspended in 25 mM Tris-HCl at pH 8.25, 5mM MgCl2. CPT enzyme activity assays contained ~100µg of desalted protein extracts from *E. coli* or ~50µg of crude yeast microsomal membrane preparations, 20µM of *trans*-FPP and 14C-IPP (50 µCi mmol-1) at a final concentration of 80µM (200 nCi) in 25 mM Tris-HCl at pH 8.25, 5mM MgCl2, 2.5 mM

Na3VO4 in a final volume of 200 µl. Assays were conducted at room temperature for 30 minutes and reaction products were hydrolyzed with HCl at a final concentration of 0.6M. Hydrolyzed products were extracted with 2.5 volumes of ethyl acetate and quantified by scintillation counting. Reaction products were applied to reverse-phase 60 Å silica plates, developed in acetone:water (39:1) and visualized by phosphorimaging. Authentic standards (C15-C120) were co-chromatographed and detected by iodine-vapor staining to determine the size of enzymatic reaction products.

Dialysis Assays

Desalted protein extracts from *E. coli* expressing SlCPT3, SlCPTBP, or both proteins together were assayed for CPT activity in 100µL chambers separated by a 5 kDa MWCO cellulose acetate membrane using Fast Micro-Equilibrium Dialyzers (Harvard Apparatus). After dialysis was complete the assay dialysates were removed from each chamber and the reaction products were extracted and analyzed as described above. TLC plates were divided into zones according to the retardation factor (*Rf*) value, scraped off, and radioactivity was quantified by scintillation counting.

ACKNOWLEDGMENTS

We thank Dr. Thomas Clemente and the University of Nebraska plant transformation facility for generating transgenic tomato plants. We also thank Dr. Jeffrey Rush (University of Kentucky) for providing the *rer2Δ* strain and native RER2 promoter, Dr. Robert Mullen (University of Guelph) for providing the pGADT7/pGBKT7 vectors and the PJ69-4A yeast strain, Dr. Jim Uniacke and Eric Clendening (University of Guelph) for technical assistance with sucrose gradient fractionation and yeast two-hybrid assays, respectively, and Greg Sobocinski (University of Michigan) for technical advice on confocal microscopy. This work was supported by grants from the USA National Science Foundation ((IOS-1025636) to E. Pichersky, from the Polish National Cohesion Strategy Innovative Economy (UDA-POIG) to E. Swiezewska, from the National Science Centre of Poland 2011/03/B/NZ1/00568 to L. Surmacz and 2012/07/B/NZ3/02437 to E. Swiezewska and from the Natural Sciences and Engineering Research Council of Canada (NSERC) to T. A. Akhtar.

SUPPORTING INFORMATION

The following materials are available in the online version of this article.

Supplemental Table S1. Synthetic oligonucleotides used in this study.

Supplemental Figure S1. Tomato leaf dolichol content is unchanged in transgenic lines with wild type SlCPT3 expression levels.

Supplemental Figure S2. Names and accession numbers of all CPT and CPTBP sequences used for phylogenetic analysis.

REFERENCES

Akhtar, T. A, Matsuba, Y., Schauvinhold, I., Yu, G., Lees, H. A, Klein, S.E. and Pichersky, E. (2013) The tomato *cis*-prenyltransferase gene family. *Plant J.* **73**, 640–652.

Apweiler, R., Hermjakob, H. and Sharon, N. (1999) On the frequency of protein glycosylation, as deduced from analysis of the SWISS-PROT database. *Biochim. Biophys. Acta.* **1473**, 4–8.

Asawatreratanakul, K., Zhang, Y., Wititsuwannakul, D., Wititsuwannakul, R., Takahashi, S., Rattanapittayaporn, A. and Koyama, T. (2003) Molecular cloning, expression and characterization of cDNA encoding *cis*-prenyltransferases from *Hevea brasiliensis*. *Eur. J. Biochem.* **270**, 4671–4680.

Bick, J.A. and Lange, B.M. (2003) Metabolic cross talk between cytosolic and plastidial pathways of isoprenoid biosynthesis: Unidirectional transport of intermediates across the chloroplast envelope membrane. *Arch. Biochem. Biophys.* **415**, 146-154.

Bajda, A., Konopka-Postupolska, D., Krzymowska, M., et al. (2009) Role of polyisoprenoids in tobacco resistance against biotic stresses. *Physiol. Plant.* **135**, 351–364.

Bugg, T. and Brandish, P. (1994) From peptidoglycan to glycoproteins: Common features of lipid-linked oligosaccharide biosynthesis. *FEMS Microbiol. Lett.* **119**, 255–262.

Chojnacki, T. and Dallnert, G. (1988) The biological role of dolichol. *Biochem. J.* **251**, 1–9.

Dai, L., Kang, G., Li, Y., Nie, Z., Duan, C. and Zeng, R. (2013) In-depth proteome analysis of the rubber particle of *Hevea brasiliensis* (para rubber tree). *Plant Mol. Biol.* **82**, 155–168.

Dudareva, N., Andersson, S., Orlova, I., Gatto, N., Reichelt, M., Rhodes, D., Boland, W. and Gershenzon, J. (2005) The nonmevalonate pathway supports both monoterpene and sesquiterpene formation in snapdragon flowers. *Proc. Natl. Acad. Sci. USA.* **102**, 933–938.

Endo, S., Zhang, Y., Takahashi, S. and Koyama, T. (2003) Identification of human dehydrodolichyl diphosphate synthase gene. *Biochim. Biophys.* **1625**, 291–295.

Foster, T.M., Lough, T.J., Emerson, S.J., Lee, R.H., Bowman, J.L., Forster, R. L. and Lucas, W.J. (2002) A surveillance system regulates selective entry of RNA into the shoot apex. *Plant Cell*, 14, 1497–1508.

Gietz, R.D. and Schiestl, R.H. (2007) High-efficiency yeast transformation using the LiAc/SS carrier DNA/PEG method. *Nat. Protoc.* **2**, 31–34.

Harrison, K.D., Miao, R.Q., Fernandez-hernándo, C., Suárez, Y., Dávalos, A. and Sessa, W.C. (2009) Nogo-B Receptor stabilizes Niemann-Pick Type C2 protein and regulates intracellular cholesterol trafficking. *Cell Metab.* **10**, 208–218.

Harrison, K.D., Park, E.J., Gao, N., Kuo, A., Rush, J.S., Waechter, C.J., Lehrman, M.A. and Sessa, W.C. (2011) Nogo–B receptor is necessary for cellular dolichol biosynthesis and protein N–glycosylation. *EMBO J.* **30**, 2490–2500.

Hemming, F.W. (1992) Dolichol: a curriculum cognitionis. *Biochem. Cell Biol.* **70**, 377-381.

Kang, J.H., Gonzales-Vigil, E., Matsuba, Y., Pichersky, E. and Barry, C.S. (2014) Determination of residues responsible for substrate and product specificity of Solanum habrochaites short-chain *cis*-prenyltransferases. *Plant Physiol.* **164**, 80–91.

Kharel, Y. and Koyama, T. (2003) Molecular analysis of *cis*–prenyl chain elongating enzymes. *Nat. Prod. Rep.* **20**, 111–118.

Kirby, J. and Keasling, J.D. (2009) Biosynthesis of plant isoprenoids: Perspectives for microbial engineering. *Annu. Rev. Plant Biol.* **60**, 335-355.

Kurisaki, A., Sagami, H. and Ogura, K. (1997) Distribution of polyprenols and dolichols in soybean plant. *Phytochemistry,* **44**, 45–50.

Lange, B.M., Rujan, T., Martin, W. and Croteau, R. (2000) Isoprenoid biosynthesis: The evolution of two ancient and distinct pathways across genomes. *Proc. Natl. Acad. U.S.A.* **97**, 13172-13177.

Liang, P.H., Ko, T.P. and Wang, A.H. (2002) Structure, mechanism, and function of prenyltransferases. *Eur. J. Biochem.* **269**, 3339–3354.

Livak, K.J. and Schmittgen, T.D. (2001) Analysis of relative gene expression data using realtime quantitative PCR and the 2-ΔΔCT Method. *Methods,* **25**, 402–408.

Miao, R.Q., Gao, Y., Harrison, K.D., Prendergast, J., Acevedo, L.M., Yu, J., Hu, F., Strittmatter, S.M. and Sessa, W.C. (2006) Identification of a receptor necessary for Nogo-B stimulated chemotaxis and morphogenesis of endothelial cells. *Proc. Natl. Acad. Sci. USA.* **103**, 10997–11002.

Nelson, B.K., Cai, X. and Nebenführ, A. (2007) A multicolored set of in vivo organelle markers for co-localization studies in *Arabidopsis* and other plants. *Plant J.* **51**, 1126–1136.

Phillips, M.A., D'Auria, J.C., Gershenzon, J. and Pichersky, E. (2008) The *Arabidopsis thaliana* type I isopentenyl diphosphate isomerases are targeted to multiple subcellular

compartments and have overlapping functions in isoprenoid biosynthesis. *Plant Cell*, **20**, 677–696.

Post, J., Deenen, N. van, Fricke, J., et al. (2012) Laticifer-specific *cis*-prenyltransferase silencing affects the rubber, triterpene, and inulin content of *Taraxacum brevicorniculatum*. *Plant Physiol.* **158**, 1406–1417.

Qu, Y., Chakrabarty, R., Tran, H.T., Kwon, E.J.G., Kwon, M., Nguyen, T.D. and Ro, D.K. (2014) A lettuce (*Lactuca sativa*) homolog of human Nogo-B receptor interacts with *cis*prenyltransferase and is necessary for natural rubber biosynthesis. *J. Biol. Chem.* (In press).

Ruiz-May, E., Kim, S.-J., Brandizzi, F. and Rose, J.K.C. (2012) The secreted plant Nglycoproteome and associated secretory pathways. *Front. Plant Sci.* **3**, 1–15.

Rush, J.S., Matveev, S., Guan, Z., Raetz, C.R.H. and Waechter, C.J. (2010) Expression of functional bacterial undecaprenyl pyrophosphate synthase in the yeast *rer2Δ* mutant and CHO cells. *Glycobiology*, **20**, 1585–1593.

Sakaihara, T., Honda, A., Tateyama, S. and Sagami, H. (2000) Subcellular fractionation of polyprenyl diphosphate synthase activities responsible for the syntheses of polyprenols and dolichols in spinach leaves. *J. Bio- chem*. **128**, 1073–1078.

Sanyal, S., Frank, C.G. and Menon, A.K. (2008) Distinct flippases translocate glycerophospholipids and oligosaccharide diphosphate dolichols across the endoplasmic reticulum. *Biochemistry*, **47**, 7937–7946.

Sanyal, S. and Menon, A.K. (2010) Stereoselective transbilayer translocation of mannosyl phosphoryl dolichol by an endoplasmic reticulum flippase. *Proc. Natl. Acad. Sci. USA.* **107**, 11289–11294.

Sato, M., Sato, K., Nishikawa, S., Hirata, A., Kato, J. and Nakano, A. (1999) The yeast RER2 gene, identified by endoplasmic reticulum protein localization mutations, encodes *cis*–prenyltransferase, a key enzyme in dolichol synthesis. *Mol. Cell. Biol.* **19**, 471–483.

Schenk, B., Fernandez, F. and Waechter, C.J. (2001) The inside and outside of dolichyl phosphate biosynthesis and recycling in the endoplasmic reticulum. *Glycobiology*, **11**, 61– 70.

Schmidt, T., Hillebrand, A., Wurbs, D., Wahler, D., Lenders, M., Schulze Gronover, C. and Prüfer, D. (2010) Molecular Cloning and Characterization of Rubber Biosynthetic Genes from *Taraxacum koksaghyz. Plant Mol. Biol. Report.* **28**, 277–284.

Shridas, P., Rush, J.S. and Waechter, C.J. (2003) Identification and characterization of a cDNA encoding a long-chain *cis*–isoprenyltranferase involved in dolichyl monophosphate biosynthesis in the ER of brain cells. *Biochem. Biophys. Res. Commun*. **312**, 1349–1356.

Skorupińska-Tudek, K., Bieńkowski, T., Olszowska, O., Furmanowa, M., Chojnacki, T., Danikiewicz, W. and Swiezewska, E. (2003) Divergent pattern of polyisoprenoid alcohols in the tissues of *Coluria geoides*: A new electrospray lonization MS approach. *Lipids*, **38**, 981–990.

Skorupinska-Tudek, K., Wojcik, J. and Swiezewska, E. (2008) Polyisoprenoid alcohols – recent results of structural studies. *Chem. Rec.* **8**, 33–45.

Stone, B.Y.K.J., Wellburn, A.R., Hemming, F.W. and Pennock, J.F. (1967) The Characterization of Ficaprenol-10, -11 and -12 from the Leaves of *Ficus elastic* (Decorative Rubber Plant). *Biochem. J.* **102**, 325–330.

Surmacz, L., Plochocka, D., Kania, M., Danikiewicz, W. and Swiezewska, E. (2014) cis-Prenyltransferase AtCPT6 produces a family of very short-chain polyisoprenoids *in planta*. *Biochim. Biophys. Acta*, **1841**, 240–250.

Surmacz, L. and Swiezewska, E. (2011) Polyisoprenoids – secondary metabolites or physiologically important superlipids? Biochem. *Biophys. Res. Commun.* **407**, 627–632.

Swiezewska, E. and Danikiewicz, W. (2005) Polyisoprenoids: structure, biosynthesis and function. *Prog. Lipid Res.* **44**, 235–258.

Tamura, K., Peterson, D., Peterson, N., Stecher, G., Nei, M. and Kumar, S. (2011) MEGA5: molecular evolutionary genetics analysis using maximum likelihood, evolutionary distance, and maximum parsimony methods. *Mol. Biol. Evol.* **28**, 2731–2739.

Wahler, D., Colby, T., Kowalski, N. a, et al. (2012) Proteomic analysis of latex from the rubber-producing plant *Taraxacum brevicorniculatum*. *Proteomics*, **12**, 901–905.

Wu, F.H., Shen, S.C., Lee, L.Y., Lee, S.H., Chan, M.T. and Lin, C.S. (2009) Tape-Arabidopsis Sandwich - a simpler *Arabidopsis* protoplast isolation method. *Plant Methods*, **5**, 16–25.

Zhang, H., Ohyama, K., Boudet, J., Chen, Z., Yang, J., Zhang, M., Muranaka, T., Maurel, C., Zhu, J.K. and Gong, Z. (2008) Dolichol biosynthesis and its effects on the unfolded protein response and abiotic stress resistance in. *Plant Cell*, **20**, 1879–1898.

FIGURE LEGENDS

Figure 1. Structures of polyprenols and dolichols. The two main types of polyisoprenoids differ in their length and hydrogenation status of their α-terminal isoprene unit. Their formation is initiated with two or three all-*trans* isoprene units at the ω-end of the molecule, to which a chain of *cis*-linked isoprene units of varying length (n = 5-24 units) is added.

Figure 2. Phylogenetic distribution and structure of CPTs. (A) Neighbor-joining phylogenetic tree of known and predicted CPTs from animals, microbes and plants. CPTs fall into four distinct groups (I-IV): the dicot (I), monocot (II) and bacterial-specific groups (III) and a fourth group (IV) that contains at least one CPT from all eukaryotes. Group V contains CPT-related proteins from eukaryotes, including the human NogoB receptor and its orthologs. Branch lengths are proportional to the number of amino acid substitutions per sequence and bootstrap values (%) of 1000 replicates are indicated next to the branches; those values of <50% are omitted. (B) Comparison of the domain architectures between CPTs and CPT-related proteins. The common core CPT domain and its conserved dimer interface are highlighted in blue and yellow, respectively. Red bars denote sets of conserved residues that are involved in catalysis and/or substrate recognition. Note the conservation of a partial CPT domain and dimer interface among the proteins in group V. TP; predicted organellar targeting peptide, SP; predicted signal peptide; TM predicted transmembrane helice. Species abbreviations: At, *Arabidopsis thaliana*; Sl, *Solanum lycopersicum*; Vv, *Vitis vinifera*; Pt, *Populus trichocarpa*; Zm, *Zea mays*; Os, *Oryza sativa*; Si, *Setaria italica*; Hb, *Hevea brasiliensis*; Sy, *Synechococcus*; Syc, *Synechocystis*; Np, *Nostoc punctiforme*; Ec, *Escherichia coli*; Mt, *Mycobacterium tuberculosis*; Sp, *Streptococcus pneumonia*; Sc, *Saccharomyces cerevisiae*; Hs, *Homo Sapiens*; Dr, *Danio rerio*.

Figure 3.RNAi-mediated knockdown of SlCPT3. (A) Quantitative RT-PCR analysis of SlCPT3 gene expression in wild type (WT) leaf tissue and in three independent RNAi lines (3-1, 3-2, 3-3). Data are the mean expression values ± SD from three biological replicates. (B) Polyisoprenoid profiles of tomato leaf tissue from wild type and from the three SlCPT3 RNAi lines (3-1, 3-2, 3- 3) described in (A). Shown are the mean values ± SD from three biological replicates. Asterisks indicate a significant difference ($p < 0.05$). (C) Phenotypic consequences of SlCPT3 knockdown on the leaf morphology. Wild type tomato leaves (left) and SlCPT3 RNAi lines (right) are shown.

Figure 4. Functional complementation of the yeast *rer2Δ* mutant. (A) SlCPT3 and the SlCPTBP were introduced into the yeast *rer2Δ* dolichol mutant alone or together and growth was assessed at the indicated temperatures. The native yeast RER2 gene and the vector alone in the *rer2Δ* mutant served as positive and negative controls, respectively. (B) Yeast CPTase enzyme activity. Yeast microsomal membranes were isolated from the above strains and CPT enzyme assays were conducted with 14C-IPP and FPP as co-substrates. Enzymatic products

were resolved by reversephase TLC. Note the production of predominantly long chain products estimated to be approximately 70-90 carbons in length by microsomes from *rer2Δ* expressing RER2 or SlCPT3 + SlCPTBP; O indicates the origin. (C) Dolichol analysis. Yeast cells from the indicated strains were analyzed for dolichol content. Note that the dolichols that accumulate in the in *rer2Δ* mutant cells containing SlCPT3 and SlCPTBP are identical to those present in the cells expressing the native RER2 protein.

Figure 5. SlCPT3 and SlCPTBP interact to form a functional dolichol synthase. (A) SlCPT3 and SlCPTBP interact in the yeast two hybrid assay. SlCPT3 and SlCPTBP were introduced into the PJ69-4A yeast strain as GAL4-activating domain (AD) and GAL4 DNA-binding domain (BD) fusion proteins, respectively. Co-transformants were serially diluted and spotted on dropout selection media (-Leu, Trp) or on dropout interaction media (-Leu, Trp, His, Ade), where growth is dependent on two-hybrid protein interactions. (B) SlCPT3 and SlCPTBP interact *in planta*. Tobacco leaves were infiltrated with *Agrobacterium tumafaciens* (LBA4404 strain) carrying expression constructs for SlCPTBP-FLAG alone or in combination with SlCPT3-Myc. FLAG tagged proteins were immunoprecipitated from crude extracts (Input) and subjected to immunoblot analysis using anti-FLAG and anti-Myc antibodies. The immunoglobulin light chain of the Anti-FLAG M2 affinity gel used for Co-IP is indicated by the asterisk. (C) Dolichol synthase enzyme activity assayed in a cell-free extract of *E. coli*. Desalted protein extracts from *E. coli* cells expressing SlCPT3, SlCPTBP, or the two proteins together were assayed for CPT activity in equilibrium dialysis chambers that were partitioned by a 5 kDa cutoff membrane. Enzymatic products were separated by reverse-phase TLC and radioactivity was measured in the zones according their retardation factor (*Rf*) value. The synthesis of dolichols (shaded region, C75-C90) were only detected in extracts containing both SlCPT3 and SlCPTBP. Note that the enzymatic reaction products readily equilibrate across dialysis membrane.

Figure 6. Subcellular localization of SlCPT3 and SlCPTBP. (A-C) SlCPT3 was fused to the mCherry fluorescent reporter (CPT3-mCherry) and transiently expressed in *Arabidopsis* mesophyll protoplasts that stably express an ER-localized GFP reporter (ER-GFP). (D-F) Similarly, SlCPTBP fused to mCherry (CPTBP-mCherry) was transiently expressed *Arabidopsis* protoplasts expressing ER-GFP. Note the co-localization of SlCPT3 and SlCPTBP with the ERGFP reporter. (G-I) CPTBP-mCherry and CPT3-GFP and were co-transformed into wild type *Arabidopsis* protoplasts. Note the overlapping fluorescent signals. (J) Sucrose density-gradient fractionation. A membrane preparation from tobacco leaves that

transiently co-express SlCPT3- myc and SlCPTBP-FLAG was fractioned through a continuous (25-55%) sucrose density gradient. Samples of each fraction were resolved by SDS-PAGE and analyzed by immunoblotting using Myc- and FLAG-specific antibodies. The distribution of subcellular marker proteins were identified with antibodies specific for BiP (ER), Arf1 (Golgi), and H+- ATPase (plasma membrane). Horizontal bars above each blot indicate the peak fractions for each protein.

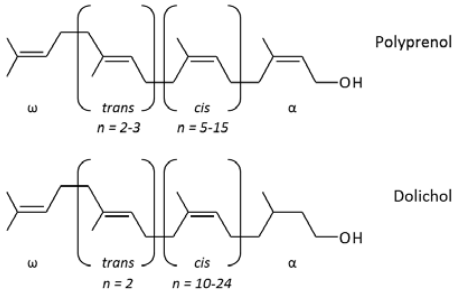

Figure 1

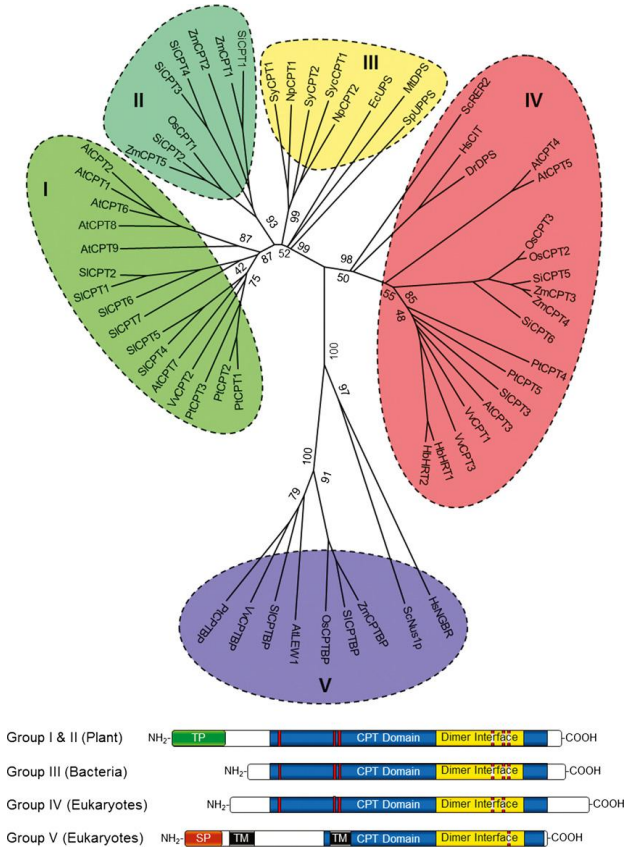
I
II
III
IV
V
AtCPT2
AtCPT1
AtCPT6
AtCPT8
AtCPT9
SlCPT2
SlCPT1
SlCPT6
SlCPT7
SlCPT5
SlCPT4
AtCPT7
VvCPT2
PtCPT3
PtCPT2
PtCPT1
SlCPT1
ZmCPT2
ZmCPT1
SlCPT4
SlCPT3
OsCPT1
SlCPT2
ZmCPT5
SyCPT1
NpCPT1
SyCPT2
SycCPT1
NpCPT2
EcUPS
MtDPS
SpUPPS
ScRER2
HsCIT
DrDPS
AtCPT4
AtCPT5
OsCPT3
OsCPT2
SlCPT5
ZmCPT3
ZmCPT4
SlCPT6
PtCPT4
PtCPT5
SlCPT3
AtCPT3
VvCPT1
VvCPT3
HbHRT1
HbHRT2
PtCPTBP
VvCPTBP
SlCPTBP
AtLEW1
OsCPTBP
SlCPTBP
ZmCPTBP
ScNus1p
HsNGBR
93
99
87
52
99
98
50
42
87
75
55
85
48
100
97
100
91
79
Group I & II (Plant)
Group III (Bacteria)
Group IV (Eukaryotes)
Group V (Eukaryotes)
NH2-
TP
SP
TM
CPT Domain
Dimer Interface
-COOH

Figure 2

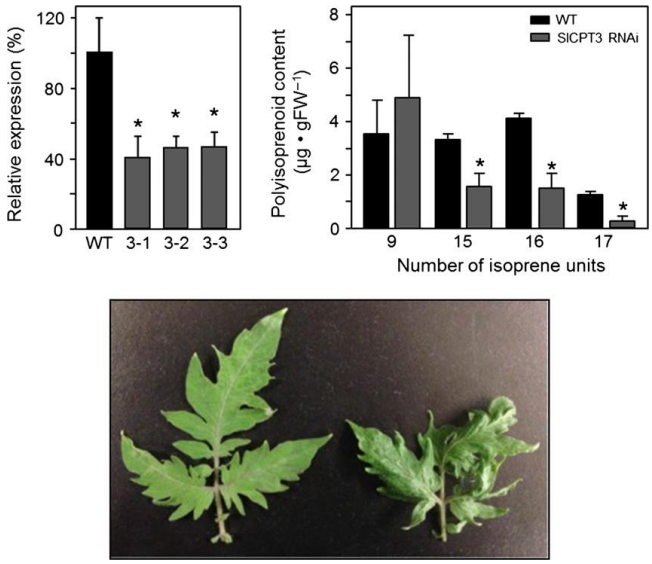
Relative expression (%)
120
80
40
0
WT
3-1
3-2
3-3
Polyisoprenoid content
(μg • gFW⁻¹)
8
6
4
2
0
WT
SlCPT3 RNAi
9
15
16
17
Number of isoprene units

Figure 3

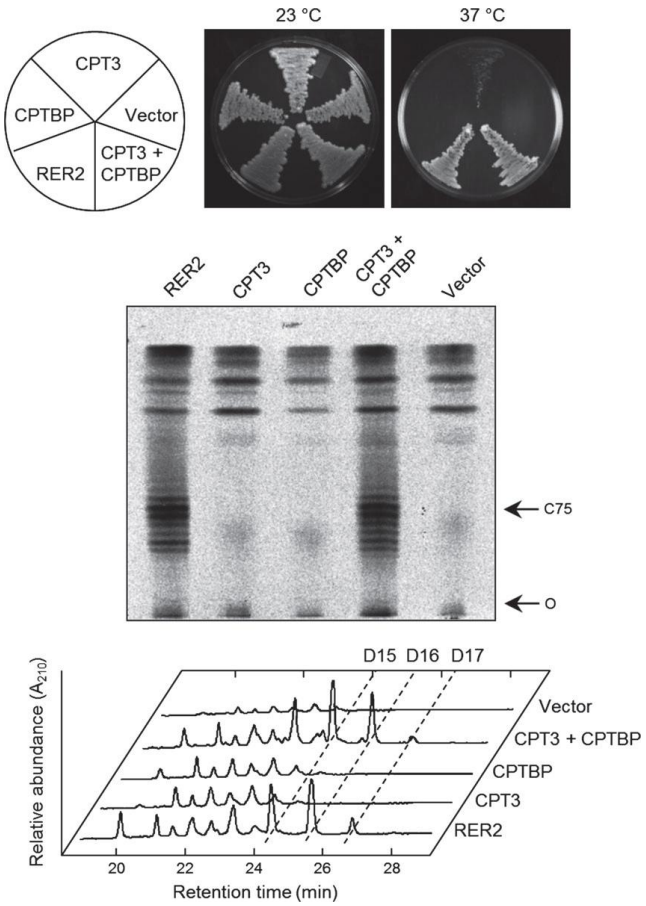
23 °C
37 °C
CPT3
CPTBP
Vector
CPT3 +
CPTBP
RER2
RER2
CPT3
CPTBP
CPT3 +
CPTBP
Vector
C75
O
D15 D16 D17
Relative abundance (A210)
Vector
CPT3 + CPTBP
CPTBP
CPT3
RER2
20
22
24
26
28
Retention time (min)

Figure 4

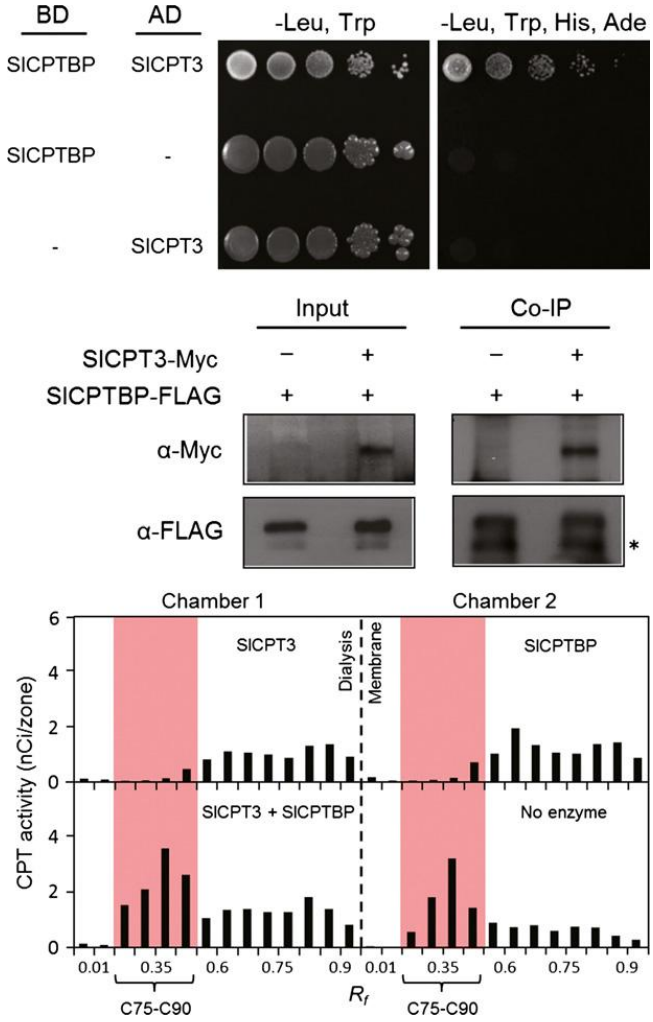
BD
AD
-Leu, Trp
-Leu, Trp, His, Ade
SlCPTBP
SlCPT3
SlCPTBP
-
-
SlCPT3
Input
Co-IP
SlCPT3-Myc
SlCPTBP-FLAG
α-Myc
α-FLAG
*
Chamber 1
Chamber 2
SlCPT3
Dialysis Membrane
SlCPTBP
SlCPT3 + SlCPTBP
No enzyme
CPT activity (nCi/zone)
C75-C90
C75-C90
R_f

Figure 5

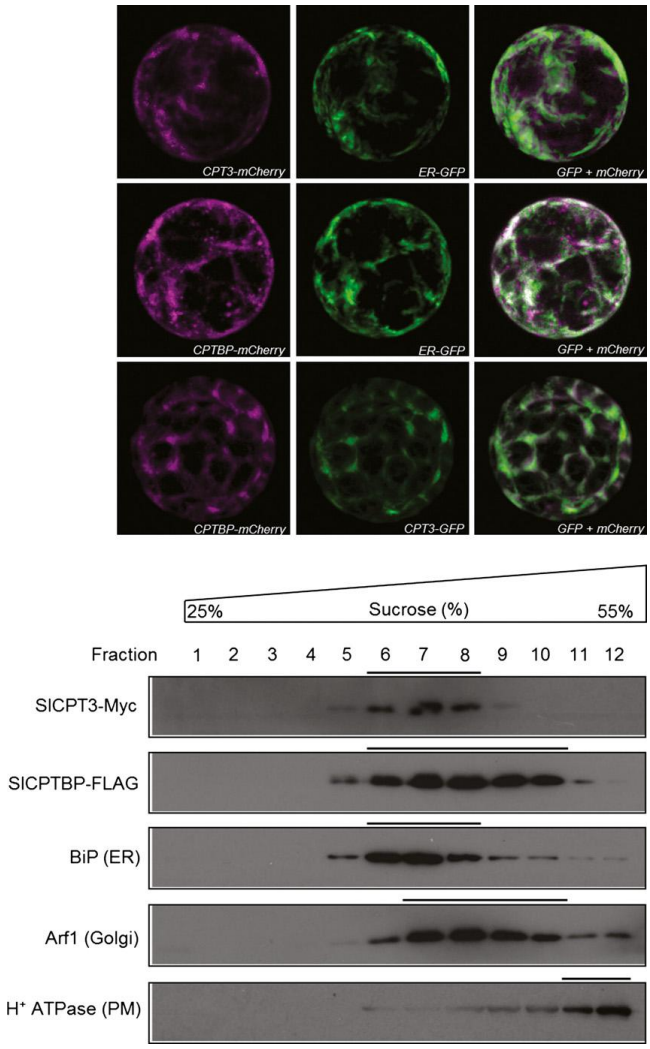
CPT3-mCherry
ER-GFP
GFP + mCherry
CPTBP-mCherry
ER-GFP
GFP + mCherry
CPTBP-mCherry
CPT3-GFP
GFP + mCherry
25%
Sucrose (%)
55%
Fraction 1 2 3 4 5 6 7 8 9 10 11 12
SlCPT3-Myc
SlCPTBP-FLAG
BiP (ER)
Arf1 (Golgi)
H+ ATPase (PM)

Figure 6